Measurements of Viscosity in Pure-Electron Plasmas

J. M. Kriesel* and C. F. Driscoll

Physics Department, University of California, San Diego, California 92093-0319

Measurements of the viscosity in quiescent magnetized pure-electron plasmas are up to 10^8 times larger than predicted by classical collisional theory. This strong viscosity is due to long-range "$\mathbf{E} \times \mathbf{B}$ drift collisions" between electrons separated by up to a Debye length. Recent theories of long-range collisions show order-of-magnitude agreement with the measurements, but do not give the observed dependence on the plasma column length. A simple empirical scaling law fits the length and magnetic field dependence surprisingly well.

            PACS numbers: 52.25.Fi, 52.27.Jt

Single-species plasmas such as pure-electron or pure-ion plasmas can be confined in a state of global thermal equilibrium using static magnetic and electric fields. The thermal equilibrium state of these non-neutral plasmas is characterized by uniform temperature, near-uniform density, and uniform rotation about the magnetic field. If the rotation has some shear, interparticle collisions cause cross-magnetic-field particle transport, which reduces the shear and brings the plasma closer to thermal equilibrium.

Measurements of the viscosity associated with this shear-driven transport test collisional transport theories [1] and also provide basic knowledge for applications which utilize non-neutral plasmas [2]. Two examples of such applications are studies of two-dimensional vortex dynamics using electron columns [3,4] and studies of Coulomb crystals using laser-cooled ion clouds [5]. For these and many other applications, an understanding of the viscosity over the wide range of gaseous, liquid, and crystal regimes [6] would be particularly beneficial.

Previous experiments [7] with pure-electron plasmas measured a global rate of relaxation toward equilibrium, $\tau_{eq}^{-1} \equiv \nu_{eq}$, which was found to be up to 10^4 times larger than predicted by "classical" Boltzmann collision theory [8,9]. In addition, ν_{eq} scaled roughly with magnetic field as $\nu_{eq} \propto B^{-1}$, rather than as the predicted B^{-4}. These previous measurements prompted new theories of collisional transport based on long-range "$\mathbf{E} \times \mathbf{B}$ drift collisions" [10–12], but did not adequately test the theories.

In this paper, we report the first measurements of the local coefficient of kinematic viscosity κ in a pure-electron plasma. These new measurements allow for an accurate comparison to collisional transport theory over a wide parameter range in the gaseous regime. Here, we vary B by a factor of 200 and the plasma length L by a factor of 10, and find that the data fit an empirical formula which scales approximately as $\kappa \propto B/L$, giving $\nu_{eq} \propto B^{-1}L^{-1}$. This measured viscosity is as much as 10^8 times larger than predicted by classical theory. In contrast, recent theories of long-range collisions are in order-of-magnitude agreement with the data, but the observed length dependence is still not understood.

The experiments [13] were conducted using two similar Penning-Malmberg traps, "EV" and "CamV" (Fig. 1). Both traps consist of a series of hollow conducting cylinders with wall radius $R_w \approx 4$ cm, in ultrahigh vacuum ($P \lesssim 10^{-10}$ Torr). Axial confinement of electrons is energetically assured by applying negative voltages ($V_c = -100$ V) to two end cylinders, and radial confinement is provided by a uniform axial magnetic field ($0.047 \leq B \leq 0.47$ kG on EV and $0.5 \leq B \leq 10$ kG on CamV). The trapped electron density is typically $n \approx 10^7$ cm^{-3}, and the thermal energy per electron is $T \approx 1$ eV. The plasma column has rounded ends, with a length ($4 \lesssim L \lesssim 44$ cm) somewhat smaller than the length between confinement cylinders, as shown in Fig. 1.

Experiments are conducted with an inject/hold/dump-and-measure cycle. A θ-symmetric electron plasma with relatively large rotational shear is created by adjusting the bias and heating voltages on a hot tungsten source [14]. The plasma is trapped and held for a time t and then dumped axially onto a Faraday cup (EV) or phosphor screen (CamV), giving the z-integrated density,

$$Q(r, t) = \int dz \, n(r, z, t). \tag{1}$$

The shot-to-shot reproducibility is better than 1%, i.e., $\delta Q/Q \lesssim 0.01$, so the density evolution can be obtained by holding nearly identical plasmas for different periods of time.
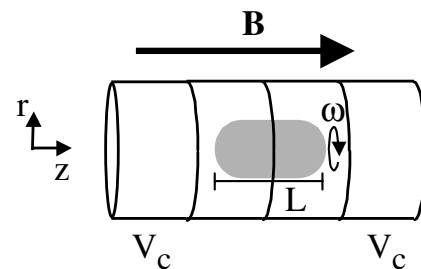

FIG. 1. Schematic of the cylindrical Penning-Malmberg trap (not all confinement cylinders are shown).

    0031-9007/01/87(13)/135003(4)$15.00

We also measure the plasma temperature T with a modified dump. The EV apparatus has a "magnetic Beach" analyzer [15], giving $T_\perp(r, t)$; whereas, in CamV a ramped-dump "evaporation" measurement [16] gives $T_\parallel(t)$ at $r = 0$ only. For these experiments, the temperature does not vary significantly with radius [13], and $T_\perp(r) \approx T_\parallel(r) \equiv T$.

We obtain the z dependence of the density $n(r, z)$ and potential $\phi(r, z)$ from a numerical solution of the 2D Poisson equation [17]. This uses the measured $Q(r)$ and T and the applied trapping voltages, and presumes local Boltzmann equilibrium along each field line, i.e., $n(r, z) \propto Q(r) \exp[-e\phi(r, z)/T]$. We then calculate the total fluid rotation as

$$\omega_{\text{tot}}(r, z) = \omega_E(r, z) + \omega_D(r, z)$$
$$= \frac{c}{Br}\left[\frac{\partial}{\partial r}\phi(r, z) - \frac{T}{en(r, z)}\frac{\partial}{\partial r}n(r, z)\right]. \quad (2)$$

The resulting $\omega_{\text{tot}}(r, z)$ is observed to be essentially constant in z even in the end sheaths [as follows analytically from local Boltzmann equilibrium if $T(r) = \text{const}$], so we consider only $\omega(r) \equiv \omega(r, 0)$. We also use the Poisson solution to define an effective plasma length as $L(r) \equiv Q(r)/n(r, 0)$.

Figures 2a and 2b show the measured density and calculated rotation profiles at three different times for one set of initial conditions in EV. Initially, at $t = 0.1$ s, the plasma has large radial variations in density, and, consequently, substantial shear in the rotation $\omega_{\text{tot}}(r)$. As time increases, some electrons move radially inward while others move outward, smoothing the density profile and decreasing the shear. The total angular momentum is conserved to within 1%, verifying that the transport is predominantly due to electron-electron interactions, as opposed to electrons interacting with an external asymmetry [18] or with neutral gas [19].

Comparisons between measurements and theories are based on a standard model of viscous transport in a cylindrically symmetric magnetized fluid [20]. In this model, viscosity acts on shears in the rotation to produce θ forces, which in turn lead to radial particle drifts. These θ forces are described by the (r, θ) component of the symmetric pressure-stress tensor **P**, given by

$$P_{r\theta}(r) = -[mn(r)\kappa(r)]r\frac{\partial\omega_{\text{tot}}(r)}{\partial r}. \quad (3)$$

The θ component of the overall force balance equation, $\nabla \cdot \mathbf{P} = -en(\mathbf{E} + \mathbf{v}/c \times \mathbf{B})$, gives the radial drift $v_r(r)$ and radial particle flux $\Gamma_r(r)$ as

$$\Gamma_r(r) \equiv n(r)v_r(r) = \frac{c}{eB}\frac{1}{r^2}\frac{\partial}{\partial r}r^2 P_{r\theta}(r). \quad (4)$$

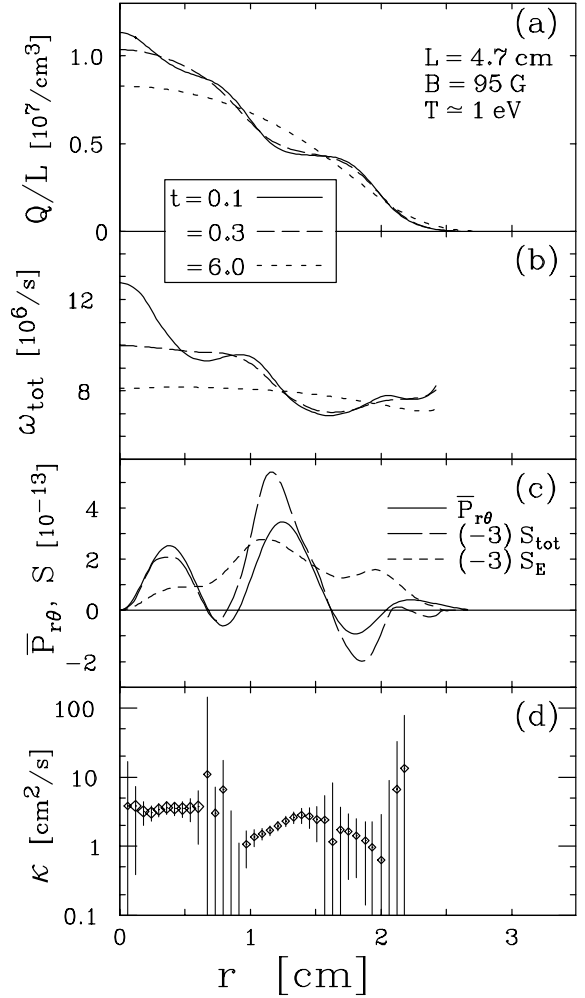Experimentally, we calculate the z-integrated radial flux from two density profiles at t_1 and t_2 as

FIG. 2. (a) Measured z-integrated electron density $Q(r)$ at 3 times. (b) Total fluid rotation $\omega_{\text{tot}}(r, 0)$ at these times. (c) Stress tensor $\overline{P}_{r\theta}(r)$ compared to shear profiles $S_{\text{tot}}(r)$ and $S_E(r)$, for the data at $t = 0.1$ and 0.3 s. (d) Kinematic viscosity $\kappa(r)$ calculated from stress $\overline{P}_{r\theta}(r)$ and total shear $S_{\text{tot}}(r)$.

$$\overline{\Gamma}_r(r) \equiv -\frac{1}{r}\int_0^r dr'\, r'\frac{Q(r', t_2) - Q(r', t_1)}{t_2 - t_1}. \quad (5)$$

The z-integrated stress follows from Eq. (4) as

$$\overline{P}_{r\theta}(r) \equiv \frac{eB}{c}\frac{1}{r^2}\int_0^r dr'\, r'^2\overline{\Gamma}_r(r'). \quad (6)$$

The measured kinematic viscosity is then obtained as the ratio of the z-integrated stress $\overline{P}_{r\theta}$ to the density-weighted total shear S_{tot} as

$$\kappa(r) \equiv \frac{\overline{P}_{r\theta}(r)}{-S_{\text{tot}}(r)} \equiv \frac{\overline{P}_{r\theta}(r)}{-mQ(r)r\partial\omega_{\text{tot}}/\partial r}. \quad (7)$$

Figure 2c shows $\overline{P}_{r\theta}(r)$ and $(-3)S_{\text{tot}}(r)$ calculated from the profiles of Figs. 2a and 2b at $t = 0.1$ and 0.3. The radial dependence of the stress qualitatively matches that of the total shear, with $\kappa \approx 3$.

Figure 2d shows the viscosity $\kappa(r)$ calculated from the ratio of $\overline{P}_{r\theta}$ and S_{tot} in Fig. 2c. The error bars for κ are determined by propagating the shot noise in $Q(r)$ and T. The

measured viscosity is relatively constant in regions where $\overline{P}_{r\theta}$ and S_{tot} are large, but has large uncertainty near the zeros of $P_{r\theta}$ and S_{tot}. Even small offsets in the zero crossings (e.g., from positional inaccuracies) can cause spurious "trends" in the data, as seen for $r = 1.0 - 1.3$ cm. More problematically, stresses from external asymmetries cause errors at large radii [13] for long plasmas with small B/L.

We therefore use averages of $\kappa(r)$ over the first "bump" of $\overline{P}_{r\theta}$ to obtain parameter scalings; that is, from $r = 0.1 - 0.6$ cm for EV data (the large symbols in Fig. 2d) and from $r = 0.2 - 0.4$ cm for CamV data. Measurements of this average viscosity in relatively short plasmas (e.g., Fig. 2) are shown in Fig. 3 as a function of B. The viscosity observed on both apparatuses increases with magnetic field roughly as $\kappa \propto B^1$.

In contrast, the classical theory of transport predicts a much smaller viscosity, scaling as $\kappa \propto B^{-2}$ as shown in Fig. 3. This theory [8,9] treats only short-range velocity-scattering collisions with impact parameters $\rho < r_c$, and gives

$$\kappa_{\text{clas}} = \frac{2\sqrt{\pi}}{5} \nu_c r_c^2 \ln(r_c/b) \propto B^{-2}L^0. \qquad (8)$$

Here $\nu_c \equiv n\overline{v}b^2 \approx 9 \text{ s}^{-1}$ is a "bare" collision frequency, $\overline{v} \equiv \sqrt{T/m} \approx 40 \text{ cm}/\mu\text{s}$ is the thermal velocity, $r_c \equiv \overline{v}/(eB/mc) \approx 24 \ \mu\text{m} \ [B/(\text{kG})]^{-1}$ is the thermal cyclotron radius, and $b \equiv e^2/T \approx 0.14 \ \mu\text{m}$ is the classical distance of closest approach. [In Eqs. (8)–(12), we display the basic scaling with B and L, ignoring logarithmic factors.]

The observed viscosity is apparently due to long-range $\mathbf{E} \times \mathbf{B}$ drift collisions with impact parameters $r_c \lesssim \rho \lesssim \lambda_D$, where $\lambda_D \equiv \sqrt{T/4\pi e^2 n} \approx 0.23$ cm is the Debye shielding length [21]. This transport was first analyzed for the 3D (or "infinite-length") regime where

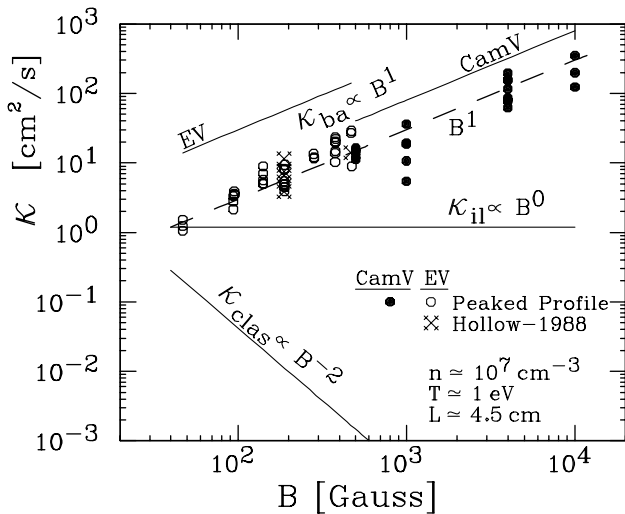FIG. 3.   Measured kinematic viscosity κ vs confining magnetic field B. The dashed line indicates a scaling of B^1; the solid lines are theory predictions for the experimental parameters.

each pair of electrons interacts only once as they stream axially past one another, giving [10,11]

$$\kappa_{\text{il}} = \frac{\sqrt{\pi}}{3} \nu_c \lambda_D^2 \ln(\overline{v}/v_{\text{min}}) \propto B^0 L^0. \qquad (9)$$

Here, v_{min} is the minimum relative axial velocity between two interacting particles (representing the maximum time for the interaction), as determined by either shears or velocity-scattering collisions. This viscosity coefficient agrees with the measurements at the lowest magnetic field, but is about 200 times smaller than the measurements at the highest field.

For short plasmas, where a thermal electron bounces many times axially before it moves substantially in (r, θ), each pair of electrons may have many correlated collisions, leading to enhanced viscosity. Two separate 2D theories have analyzed this enhancement by treating electrons as magnetic-field-aligned "rods" of charge moving in (r, θ). The first 2D analysis [12] predicted that enhanced viscosity is driven by shears in just the $\mathbf{E} \times \mathbf{B}$ rotation $\omega_E(r)$, and that the enhancement occurs only in nonmonotonic rotation profiles.

However, the present experiments show that there is no substantial difference between the measured viscosity for a hollow (nonmonotonic) density profile and that for a peaked profile [13]. For example, Figure 3 shows the close agreement between recent data from peaked profiles (e.g., Fig. 2) and the few points from a previous data set [7] labeled "Hollow-1988" which were of sufficient completeness to yield a viscosity coefficient. Additionally, for both peaked and hollow profiles [13], the viscous stress correlates much more closely with shears in $\omega_{\text{tot}}(r)$ than with shears in $\omega_E(r)$. For example, the measured $S_E(r) \equiv mQ(r)r\partial\omega_E/\partial r$ in Fig. 2c does not change sign nor does it vary as strongly as do $\overline{P}_{r\theta}(r)$ and $S_{\text{tot}}(r)$.

In contrast, a more recent 2D "bounce-averaged" theory [22] includes an approximation to the drifts due to thermal electron penetration into the end sheaths, and predicts enhanced transport driven by shears in the total fluid rotation $\omega_{\text{tot}}(r)$ for both monotonic and hollow profiles. The predicted viscosity is

$$\kappa_{ba} = 16\pi^2 \nu_c d^2 N_b g(2d/r) \propto B^1 L^{-3}, \qquad (10)$$

where

$$N_b \equiv \frac{f_b}{r\omega_E'} \equiv \frac{\overline{v}/2L}{r\omega_E'} \propto \frac{B}{L} \qquad (11)$$

is the effective number of axial bounces a thermal particle executes before being sheared away from neighboring particles, $d \equiv \overline{v}r_c|L'/L| \, |r\omega_E'|^{-1} = 2r_cL'/N_b$ is the predicted radial interaction distance, $g(2d/r) \approx 0.1$ is an integral that is calculated numerically, and primes denote $(\partial/\partial r)$. This theory is shown as two separate lines in Fig. 3, since the detailed dependence on ω_E' and L' differs for the EV and CamV initial conditions. The predicted viscosity for these short plasmas is 3–10 times larger than observed.
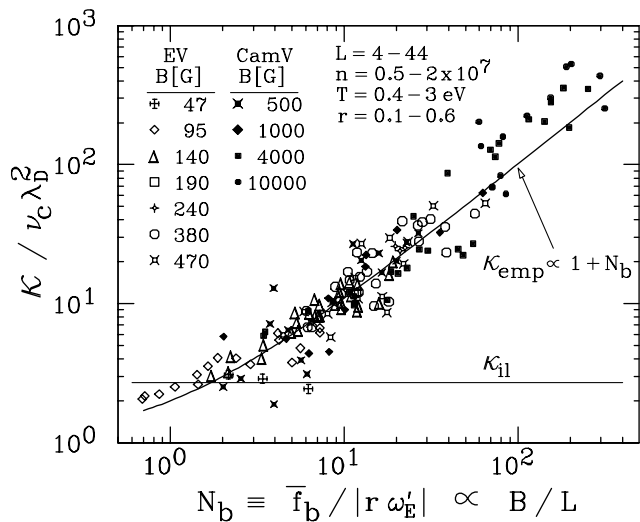
FIG. 4. Measured viscosity κ vs the effective number of bounces N_b. The solid curve shows the simple empirical formula of Eq. (12).

The most counterintuitive aspect of the present results is that the viscosity depends on the plasma length in addition to the magnetic field. The measured viscosity decreases approximately as $\kappa \propto L^{-1}$ as the length is increased from 4 to 44 cm. Empirically, we find that the parameter N_b alone characterizes both the B and L dependence rather accurately: All of the data on both machines is well described by the simple empirical formula,

$$\kappa_{\mathrm{emp}} \equiv (1 + N_b)\nu_c\lambda_D^2 \propto B^1 L^{-1}. \tag{12}$$

The accuracy of this empirical formula is shown in Fig. 4, which displays the scaled viscosity $\kappa/\nu_c\lambda_D^2$ versus N_b.

For long plasmas and/or low magnetic fields, with $N_b \lesssim 1$, the measured data show factor of 2 agreement with the 3D infinite-length theory of long-range collisions. In this regime, the radial shears apparently separate the interacting particles and prevent multiple correlated collisions. For short plasmas and/or high fields, with $N_b \gg 1$, the measured viscosity is enhanced by an amount that scales as N_b, apparently due to multiple correlated collisions. However, the theory analysis is still inadequate: While the parameter N_b does appear in the 2D bounce-averaged prediction of Eq. (10), the other shear and length dependencies in the d^2 term are not supported by the data. (This theory is not displayed in Fig. 4 due to the choice of axes and wide variation in d^2.) As a caveat, we note that further experiments may establish dependencies (such as density or temperature) not included in κ_{emp}.

Other experiments with pure ion plasmas have measured transport coefficients for test particle diffusion [23] and heat conduction [24], but only in the $N_b \lesssim 1$ regime where multiple collisions and finite-length effects are presumably negligible. Both of these measurements agree quantitatively with the 3D infinite-length theory of long-range collisions. Recently, a 2D bounce-averaged analysis

of test particle diffusion [25] has been developed for the regime $N_b \gg 1$, and ion experiments may soon be able to access this 2D regime using extremely short plasmas. It remains to be seen whether understanding finite-length effects in the somewhat simpler case of diffusion will contribute to a deeper understanding of the viscosity results presented here.

*Current address: Time and Frequency Division, NIST, 325 Broadway, Boulder, CO 80305.

[1] For a summary of collisional transport in non-neutral plasmas, see D. H. E. Dubin, Phys. Plasmas **5**, 1688 (1998).
[2] For recent results, see *Non-Neutral Plasma Physics III,* edited by J. J. Bollinger, R. Spencer, and R. Davidson, AIP Conf. Proc. No. 331 (AIP, New York, 1999).
[3] K. S. Fine *et al.,* Phys. Rev. Lett. **75**, 3277 (1995).
[4] D. Durkin and J. Fajans, Phys. Rev. Lett. **85**, 4052 (2000).
[5] J. J. Bollinger *et al.,* Phys. Plasmas **7**, 7 (2000).
[6] D. H. E. Dubin and T. M. O'Neil, Rev. Mod. Phys. **71**, 87 (1999).
[7] C. F. Driscoll, J. H. Malmberg, and K. S. Fine, Phys. Rev. Lett. **60**, 1290 (1988).
[8] C. L. Longmire and M. N. Rosenbluth, Phys. Rev. **103**, 507 (1956).
[9] T. M. O'Neil and C. F. Driscoll, Phys. Fluids **22**, 266 (1979).
[10] T. M. O'Neil, Phys. Rev. Lett. **55**, 943 (1985).
[11] D. H. E. Dubin (personal communication). A recalculation gives the K of Ref. [10] [Eq. (13)] increased by a factor of 2.
[12] D. H. E. Dubin and T. M. O'Neil, Phys. Rev. Lett. **60**, 1286 (1988).
[13] J. M. Kriesel, Ph.D. thesis, University of California, San Diego, 1999.
[14] J. M. Kriesel and C. F. Driscoll, Phys. Plasmas **5**, 1265 (1998).
[15] A. W. Hyatt, Ph.D. thesis, University of California, San Diego, 1988.
[16] D. L. Eggleston *et al.,* Phys. Fluids B **4**, 3432 (1992).
[17] E. H. Chao *et al.,* in Ref. [2], p. 461.
[18] J. M. Kriesel and C. F. Driscoll, Phys. Rev. Lett. **85**, 2510 (2000).
[19] E. H. Chao *et al.,* Phys. Plasmas **7**, 831 (2000).
[20] C. F. Driscoll, Phys. Fluids **25**, 97 (1982).
[21] R. C. Davidson, *Physics of Non-Neutral Plasmas* (Addison-Wesley, Redwood City, CA, 1990), p. 59.
[22] D. H. E. Dubin and T. M. O'Neil, Phys. Plasmas **5**, 1305 (1998).
[23] F. Anderegg *et al.,* Phys. Rev. Lett. **78**, 2128 (1997); D. H. E. Dubin, Phys. Rev. Lett. **79**, 2678 (1997).
[24] E. M. Hollmann, F. Anderegg, and C. F. Driscoll, Phys. Rev. Lett. **82**, 4839 (1999); D. H. E. Dubin and T. M. O'Neil, Phys. Rev. Lett. **78**, 3868 (1997).
[25] D. H. E. Dubin and D. Z. Jin, Phys. Lett A **284**, 112 (2001).